

# Tuning the Activation Threshold of a Kinase Network by Nested Feedback Loops

Quincey A. Justman,<sup>1,2\*</sup> Zach Serber,<sup>3†</sup> James E. Ferrell Jr.,<sup>3</sup> Hana El-Samad,<sup>4‡</sup> Kevan M. Shokat<sup>2‡</sup>

Determining proper responsiveness to incoming signals is fundamental to all biological systems. We demonstrate that intracellular signaling nodes can tune a signaling network's response threshold away from the basal median effective concentration established by ligand-receptor interactions. Focusing on the bistable kinase network that governs progesterone-induced meiotic entry in *Xenopus* oocytes, we characterized glycogen synthase kinase-3 $\beta$  (GSK-3 $\beta$ ) as a dampener of progesterone responsiveness. GSK-3 $\beta$  engages the meiotic kinase network through a double-negative feedback loop; this specific feedback architecture raises the progesterone threshold in correspondence with the strength of double-negative signaling. We also identified a marker of nutritional status, L-leucine, which lowers the progesterone threshold, indicating that oocytes integrate additional signals into their cell-fate decisions by modulating progesterone responsiveness.

To respond to environmental cues appropriately, biological systems establish precise response thresholds. It is unclear how metazoan signal transduction networks exert control over sensitivity because stimulus and response are separated in space and time: Rapid receipt of the signal often occurs extracellularly, whereas downstream responses occur on longer time scales and require cellwide coordination.

Maturation of *Xenopus* oocytes, the irreversible, progesterone-induced resumption of meiosis I (1, 2), provides a classic example of a

cell-fate decision with a well-defined threshold: Oocytes treated with a sufficient concentration of progesterone undergo maturation, whereas those treated with a lower concentration do not. Suprathreshold progesterone stimulus up-regulates the translation and gradual accumulation of the protein kinase Mos through a largely unidentified pathway. Mos is the essential initiator of meiosis (3); it signals through the mitogen-activated protein kinase (MAPK) cascade (composed of Mos, the MAPK kinase MEK1, and p42 MAPK) and promotes the activation of the cyclin-dependent kinase 1

(Cdk1)•cyclin B complex (Fig. 1A). Nonlinearity in the relationship between Mos concentration and MAPK activation conveys switchlike character to the decision to mature (4). In mature, M-phase cells, high Mos concentrations are maintained by continual Mos translation. Mos translation, in turn, is critically dependent on the activities of Mos, MEK, MAPK, and Cdk1, forming a positive feedback loop (5). The net effect of this nonlinearity and positive feedback is to enforce a stable separation of interphase and M phase at steady state. Thus, *Xenopus* oocyte maturation is bistable (4, 5). An oocyte crosses its progesterone threshold when Mos concentrations are sufficient to initiate M-phase positive feedback, hours after the signal is received at the cell surface. We explain how oocytes specify the progesterone concentration that initiates M-phase entry.

Depending on environmental factors and a frog's physiology, the dose of hormone required

<sup>1</sup>Graduate Group in Biophysics, University of California, San Francisco, CA 94158, USA. <sup>2</sup>Howard Hughes Medical Institute and Department of Cellular and Molecular Pharmacology, University of California, San Francisco, CA 94158, USA. <sup>3</sup>Department of Chemical and Systems Biology, Stanford University School of Medicine, Stanford, CA 94305–5174, USA. <sup>4</sup>Department of Biochemistry and Biophysics, University of California, San Francisco, CA 94158, USA.

\*Present address: Department of Molecular and Cellular Biology, Harvard University, Cambridge, MA 02138, USA.

†Present address: Amyris Biotechnologies, Incorporated, Emeryville, CA 94608, USA.

‡To whom correspondence should be addressed. E-mail: helsamad@biochem.ucsf.edu (H.E.); shokat@cmp.ucsf.edu (K.M.S.)

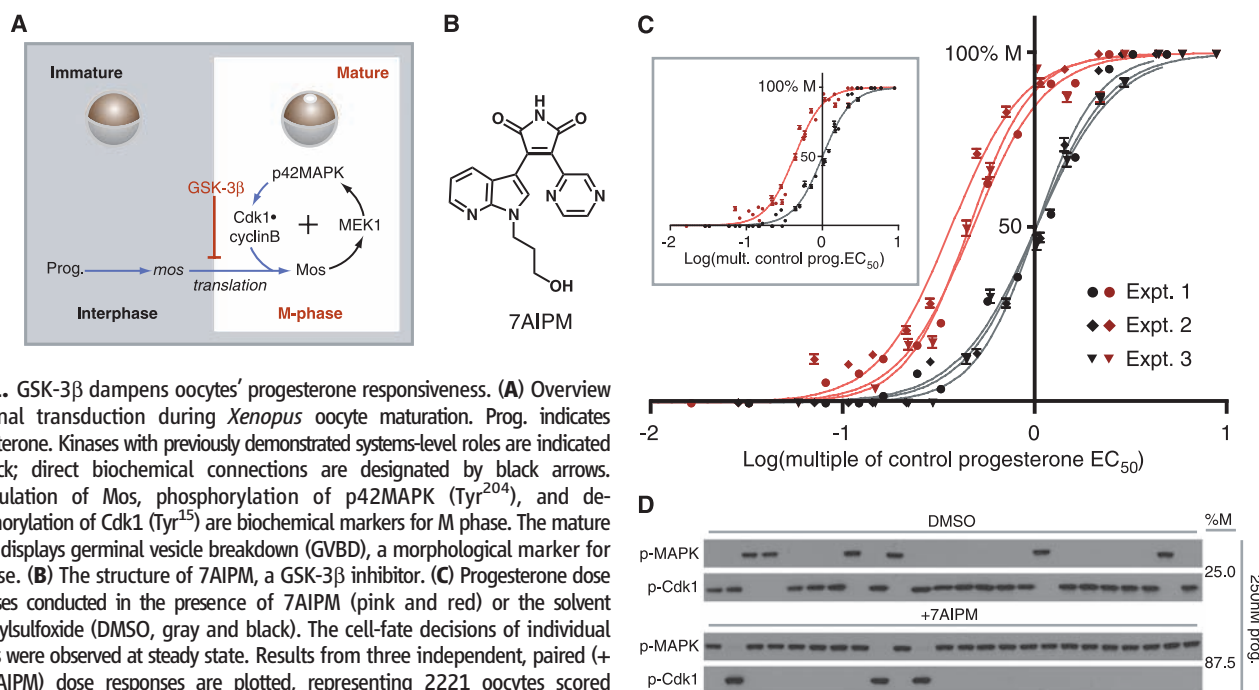


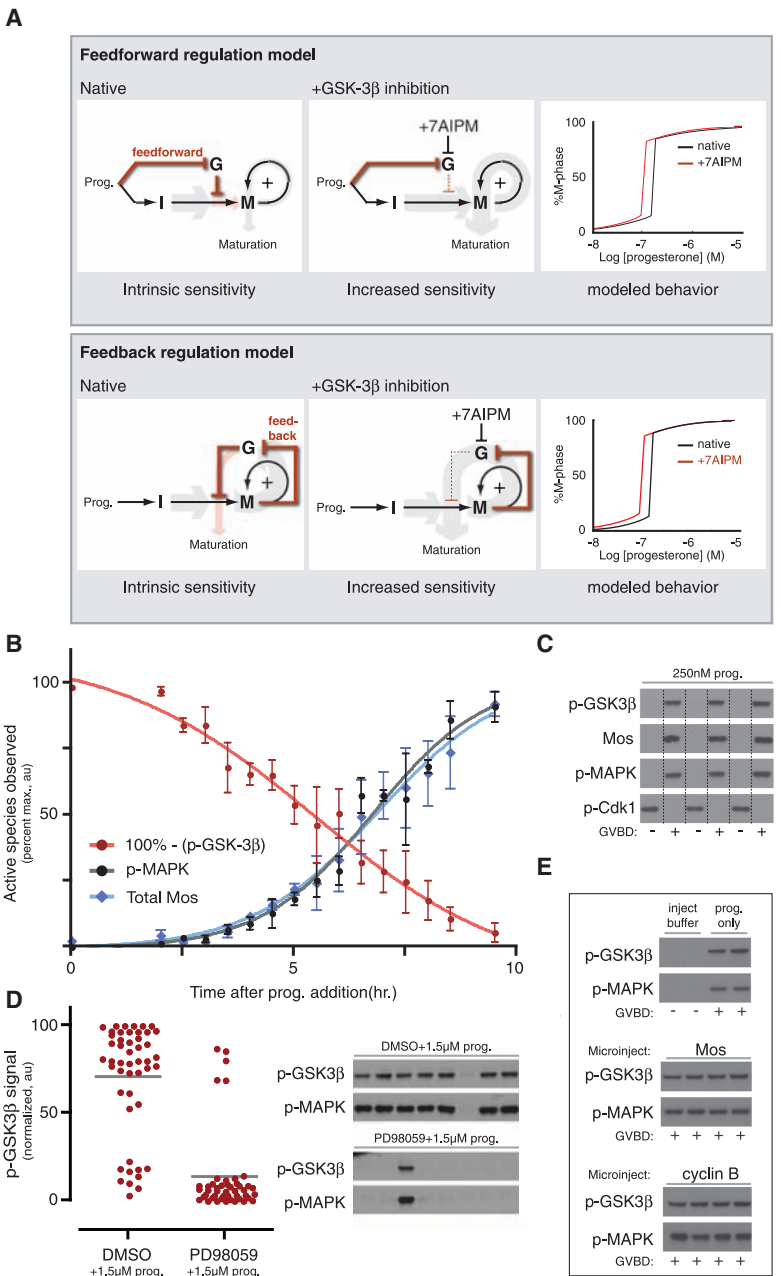
**Fig. 1.** GSK-3 $\beta$  dampens oocytes' progesterone responsiveness. **(A)** Overview of signal transduction during *Xenopus* oocyte maturation. Prog. indicates progesterone. Kinases with previously demonstrated systems-level roles are indicated in black; direct biochemical connections are designated by black arrows. Accumulation of Mos, phosphorylation of p42MAPK (Tyr<sup>204</sup>), and dephosphorylation of Cdk1 (Tyr<sup>15</sup>) are biochemical markers for M phase. The mature oocyte displays germinal vesicle breakdown (GVBD), a morphological marker for M phase. **(B)** The structure of 7AIPM, a GSK-3 $\beta$  inhibitor. **(C)** Progesterone dose responses conducted in the presence of 7AIPM (pink and red) or the solvent dimethylsulfoxide (DMSO, gray and black). The cell-fate decisions of individual oocytes were observed at steady state. Results from three independent, paired (+ or -7AIPM) dose responses are plotted, representing 2221 oocytes scored individually (error bars represent SE). For non-normalized dose responses see (8). (Inset) Composite progesterone dose responses from the three independent experiments shown in (C). For DMSO-treated oocytes (gray and black), EC<sub>50</sub> = 1.00 (normalized) and  $n_H$  = 2.3. For 7AIPM-treated oocytes (pink and red), EC<sub>50</sub> = 0.43 (normalized to DMSO control) and  $n_H$  = 2.3. **(D)** Representative single-oocyte Western blots. Each lane contains lysate prepared from one oocyte at steady state.

to induce ovulation can vary. We reasoned that, although receptor number and ligand affinity establish a basal median effective concentration (EC<sub>50</sub>) for the system, specific intracellular kinases might tune the oocytes' progesterone thresholds. Progesterone-dependent inactivation of glycogen synthase kinase-3β (GSK-3β) (by phosphorylation on Ser<sup>9</sup>) is an obligatory step in determining the cell-fate of the oocyte. Overexpression of GSK-3β can prevent progesterone-induced translation of Mos (6), and it uncoupled MAPK and Cdk1 activation, rendering M-phase entry incomplete (fig. S1). Because it regulates the transition between interphase and M phase, we tested whether GSK-3β also regulates the progesterone threshold of *Xenopus* oocytes. We measured progesterone dose re-

sponses in the presence and absence of 7-azaindoly-pyrazinyl-maleimide (7AIPM), a specific GSK-3β inhibitor (7) (Fig. 1B), and observed that constant inhibition of GSK-3β doubled the system's responsiveness to progesterone (Fig. 1C and fig. S2) (8). Single-cell experiments indicated that maturation retained its all-or-none, irreversible character in 7AIPM-treated oocytes (Fig. 1D and fig. S3), suggesting that GSK-3β dampens overall progesterone responsiveness by raising the thresholds of individual oocytes. The 7AIPM treatment brought the oocytes' in vitro EC<sub>50</sub> closer to the low nM progesterone concentrations measured in intact *Xenopus* ovaries (9, 10). We envisioned two possible threshold regulation mechanisms that center on two negative reg-

ulatory connections placed in series. First, GSK-3β could dampen interphase signaling until GSK-3β is inactivated by progesterone-dependent signaling in a feed-forward manner, before meiotic entry (Fig. 2A, top). Alternatively, M-phase feedback could inactivate GSK-3β and relieve its repression of Mos translation as the meiotic switch activates (Fig. 2A, bottom). To verify that these mechanisms can raise a bistable system's threshold, we modeled them mathematically and mimicked 7AIPM treatment by setting GSK-3β activity to zero (11). This analysis revealed that both mechanisms provide a general solution for dampening a system's responsiveness (Fig. 2A, far right). In an analytical treatment, we proved mathematically that a raised threshold is a structural feature of bistable systems con-

**Fig. 2.** GSK-3β inactivation is an M-phase event. **(A)** Feed-forward versus feedback models for GSK-3β-dependent progesterone desensitization, relating the activity of GSK-3β (G) to interphase (I) and M-phase (M) signaling. Relative signal strength (i.e., the amount of downstream, promeiosis signal per unit of progesterone) is indicated by the thickness of the gray and pink arrows. The pink arrow designates the threshold-regulation step. (Right) The black curve models the input dose-response curve of the native bistable system; the red curve models the response after 7AIPM treatment. **(B)** Time course of phosphoregulation and Mos accumulation during maturation. Average phospho-MAPK, phospho-GSK-3β, and total Mos were quantified by Western blotting (error bars are ±SD, *n* = approximately 24 oocytes per time point). At 9.5 hours, GVBD was 100%. **(C)** Single-oocyte Western blots at intermediate progesterone. Lysates were prepared from individual oocytes at steady state, then Western blotted. Lanes were assigned by cell morphology (+ indicates GVBD was observed; −, GVBD was not observed); lane lines are included for clarity. **(D)** MEK inhibition before progesterone stimulus. Lysate was prepared from individual oocytes at steady state. (Left) Phospho-GSK-3β signal quantitated by closed-circuit device (CCD) camera. Dots represent signal from single oocytes; lines indicate population average. PD98059 pretreatment reduces average GSK-3β Ser<sup>9</sup> phosphorylation significantly (*P* < 0.0001, Student's *t* test). (Right) Phospho-MAPK and phospho-GSK in representative single oocytes. Phospho-MAPK is a direct readout of MEK activity and M-phase entry. DMSO pretreatment: 71.2% M phase; PD98059 pretreatment: 10.9% M phase. Total *n* = 48 (DMSO) and 46 (PD98059). **(E)** Phospho-GSK-3β and phospho-MAPK in oocytes microinjected with Mos or nondegradable cyclin B1 (Δ90). Oocytes were lysed individually after GVBD; lysates were run on the same gel and Western blotted on a single blot. Microinjected oocytes were not stimulated with progesterone.



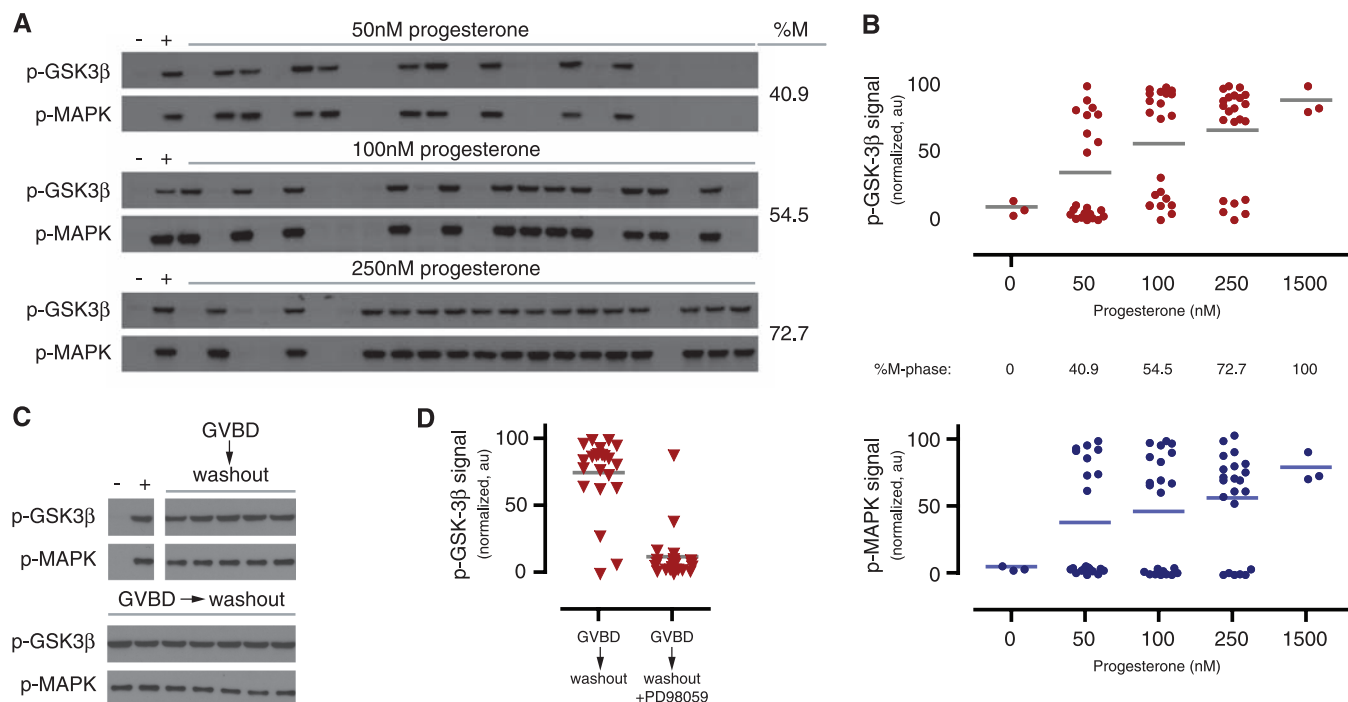


**Fig. 3.** M-phase GSK-3 $\beta$  inactivation is switchlike, MEK-dependent, and irreversible. **(A and B)** Phosphorylation of GSK-3 $\beta$  in single oocytes. Phospho-GSK-3 $\beta$  within each oocyte was scored by Western blot **(A)** then quantitated by CCD camera **(B)**, top, red. Lanes indicated by “+” were treated with 1.5  $\mu$ M progesterone. Dots represent the phospho-GSK-3 $\beta$  signal from individual oocytes; lines indicate the oocyte population’s average phospho-GSK-3 $\beta$  signal. The single-cell quantitation of MAPK phosphorylation is included for reference **(B)**,

bottom, blue. **(C and D)** Progesterone removal. After GVBD, oocytes were washed extensively over 18 hours then lysed individually. Phospho-GSK-3 $\beta$  was scored by Western blot **(C)**, a representative oocyte, total  $n = 23$ . In **(D)**, PD98059 was added during the washout period. PD98059 treatment during M-phase arrest reduces average GSK-3 $\beta$  Ser<sup>9</sup> phosphorylation significantly ( $P < 0.0001$ , Student’s  $t$  test). DMSO treatment: 86.4% M phase; PD98059 treatment: 4.2% M phase.

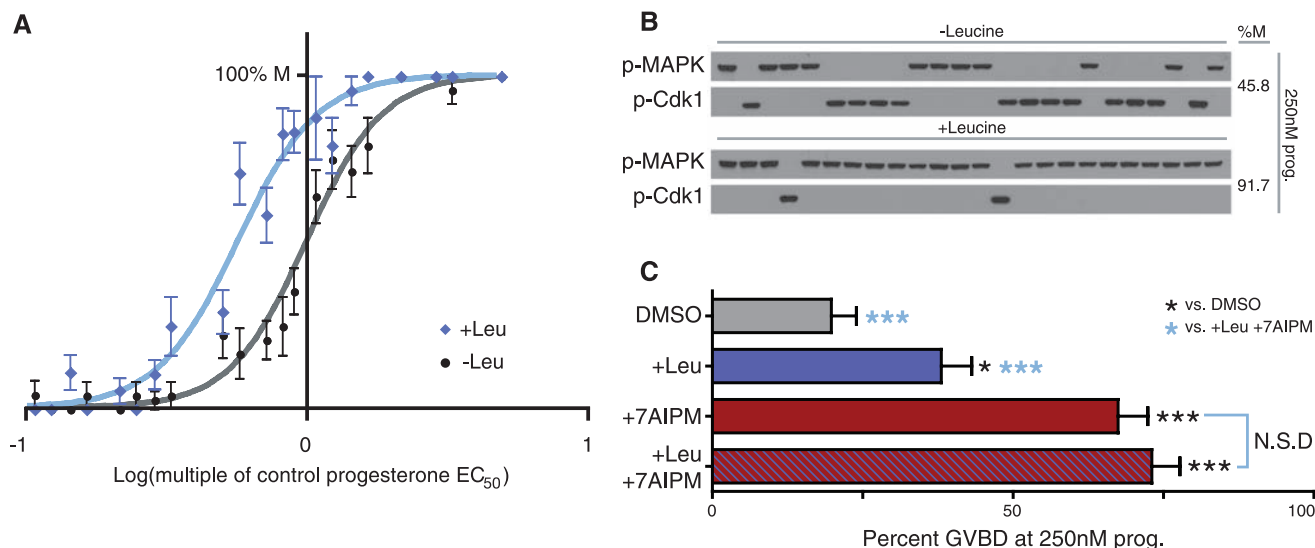


**Fig. 4.** Integration of progesterone and Leu signaling. **(A)** Progesterone dose responses of oocytes incubated in the presence of Leu (blue) or its absence (gray and black). The cell-fate decisions of individual oocytes were observed at steady state. Results plotted represent 1290 oocytes scored individually (error bars represent SE). For control (gray and black),  $EC_{50} = 1.00$  (normalized) and  $n_H = 3.2$ . For Leu-treated oocytes (blue),  $EC_{50} = 0.57$  (normalized to control) and  $n_H = 3.1$ . **(B)** Representative single-cell Western blots reveal response of individual oocytes to progesterone at

steady state, + or -Leu. **(C)** Combined treatment with Leu and 7AIPM. Oocytes were treated with DMSO ( $n = 91$ ), Leu ( $n = 92$ ), 7AIPM ( $n = 89$ ), or Leu plus 7AIPM ( $n = 89$ ) before progesterone stimulus. Cell-fate decisions were scored at steady state. Error bars represent SE. Pairwise comparisons were made to the DMSO control (black asterisks) and the +Leu+7AIPM treatment (blue asterisks),  $*P < 0.05$ ;  $***P < 0.0001$ ; “N.S.D” indicates no significant difference (Student’s  $t$  tests). More stringent  $\chi^2$  analysis reveals that all values are statistically different except 7AIPM and 7AIPM+Leu.

taining two negative regulatory connections placed in series; this is not dependent on parameter choice (fig. S8) (8).

To distinguish between these threshold regulation mechanisms, we experimentally defined GSK-3 $\beta$ 's position in the progesterone-responsive signaling network relative to M-phase entry. Unlike most kinases, phosphorylation of GSK-3 $\beta$  on Ser<sup>9</sup> inhibits its activity; this occurs through pseudo-substrate inhibition (12). We conducted a time course of phospho-GSK-3 $\beta$  accumulation at high progesterone concentration and found that maximum GSK-3 $\beta$  phosphorylation occurred during M phase (Fig. 2B) (13). Accordingly, phosphorylation of GSK-3 $\beta$  correlated precisely with the decision to enter M phase in individual progesterone-stimulated oocytes (Fig. 2C). To determine whether M-phase signaling is necessary for phosphorylation of GSK-3 $\beta$ , we initiated maturation in the presence of PD98059, a specific MEK inhibitor. PD98059 treatment significantly reduced the population's average amount of phospho-GSK-3 $\beta$  (Fig. 2D, left); single-oocyte analysis revealed a precise correlation between MEK inhibition, very low amounts of phospho-GSK-3 $\beta$ , and failure of most cells to enter M phase (Fig. 2D, right). To verify that GSK-3 $\beta$  is not inactivated by progesterone-dependent interphase signals, we initiated meiosis in the absence of progesterone by microinjecting oocytes with Mos or nondegradable cyclin B1 ( $\Delta$ 90). In the microinjected cells, phospho-MAPK confirmed meiotic entry, and phosphorylation of GSK-3 $\beta$  was indistinguishable from progesterone-treated controls (Fig. 2E), suggesting that signals originating within the M-phase feedback loop are sufficient to inactivate GSK-3 $\beta$ . Given these data, we hypothesized that GSK-3 $\beta$  regulates oocytes' progesterone responsiveness by participating in M-phase network itself.

We tested whether phosphorylation of GSK-3 $\beta$  mirrors the hallmark characteristics of MAPK activation during *Xenopus* oocyte maturation: nonlinear progesterone dependence and hysteresis (4, 5). In equivalently stimulated cells, phosphorylation of GSK-3 $\beta$  on Ser<sup>9</sup> was either nearly undetectable or maximal at steady state (Fig. 3, A and B top). No intermediate responses were observed in single cells, demonstrating that GSK-3 $\beta$  phosphorylation is ultrasensitive with respect to progesterone concentration. In mature oocytes, positive, Mos-dependent feedback is sufficiently strong to maintain meiotic commitment after progesterone is removed (5). If GSK-3 $\beta$  inactivation relies on the same M-phase feedback, GSK-3 $\beta$ 's phosphoregulation should display the same extreme hysteresis. We observed that phosphorylation of GSK-3 $\beta$  was sustained at its maximum 18 hours after removal of progesterone (Fig. 3C). Moreover, this hysteresis depended on the activity of MEK: When PD98059 was added as progesterone was removed, phosphorylation of GSK-3 $\beta$  was significantly reduced (Fig. 3D). In total, our data show that induction and maintenance of

GSK-3 $\beta$  inactivation requires feedback through the meiotic kinase network. GSK-3 $\beta$  also displays the same bistable behavior observed in MAPK and Cdk1. Taken together, these results define GSK-3 $\beta$  as a node in a MEK-dependent, double-negative feedback loop that is likely driven by the bistable, positive feedback within M-phase oocytes. These results provide experimental verification of our feedback regulation mechanism (Fig. 2A, bottom images).

GSK-3 $\beta$ -dependent desensitization might allow a cell to integrate several signals, an impossibility if it were maximally responsive to progesterone alone. The branched-chain amino acid L-leucine (Leu), a nutritional marker, regulates translation through kinases that require inhibition of GSK-3 $\beta$  for activity (14, 15). To test whether Leu-dependent signals can be integrated into oocytes' decision to mature, we conducted progesterone dose-responses in the presence and absence of extracellular Leu. Although Leu does not alter oocytes' baseline response at low progesterone concentrations (Fig. 4A), Leu lowered the oocytes' progesterone threshold, demonstrating cooperation between nutritional signals and cell-cycle entry (Fig. 4, A and B). If Leu signaling and GSK-3 $\beta$  form a common pathway during maturation, simultaneous treatment with Leu and 7AIPM would have no greater effect on progesterone threshold than either 7AIPM or Leu alone. However, if nutrient signaling was mediated through a GSK-3 $\beta$ -independent pathway, the two stimuli would have an additive or synergistic effect. We observed that the effect of Leu and 7AIPM together on progesterone responsiveness was statistically indistinguishable from that of 7AIPM alone (Fig. 4C), suggesting that GSK-3 $\beta$  regulation is a point of signal integration during *Xenopus* oocyte maturation.

Much attention has focused on the ubiquity of simple dynamical motifs in biological systems (16–23). Here, we demonstrate that layering apparently redundant motifs (positive feedback and double-negative feedback) tunes a bistable system's response threshold. This illustrates a remarkable separation of functions in bistable systems: Input EC<sub>50</sub> is regulated by relationships that are not strictly input-dependent. A striking number of biological networks contain nested feedback loops (17–19, 21), suggesting that this may be a general mechanism for modulating biological responsiveness. If multiple stimuli act on components of linked feedback loops, cells may tune their responsiveness to respond appropriately to their environment.

#### References and Notes

1. A. R. Nebreda, I. Ferby, *Curr. Opin. Cell Biol.* **12**, 666 (2000).
2. T. Kishimoto, *Curr. Opin. Cell Biol.* **15**, 654 (2003).
3. F. Gebauer, J. D. Richter, *Bioessays* **19**, 23 (1997).
4. J. E. Ferrell Jr., E. M. Machleder, *Science* **280**, 895 (1998).
5. W. Xiong, J. E. Ferrell Jr., *Nature* **426**, 460 (2003).

6. M. Sarkissian, R. Mendez, J. D. Richter, *Genes Dev.* **18**, 48 (2004).
7. D. J. O'Neill et al., *Bioorg. Med. Chem.* **12**, 3167 (2004).
8. Materials and methods are available as supporting material on Science Online.
9. L. B. Lutz et al., *Proc. Natl. Acad. Sci. U.S.A.* **98**, 13728 (2001).
10. J. E. Fortune, *Dev. Biol.* **99**, 502 (1983).
11. The feed-forward model is given by

$$\frac{dM}{dt} = k_{\text{off}}^M M^* - \gamma_M M - k_{\text{on}}^M M + \frac{f_{\text{pos}} \frac{M^{*n_H}}{M^{*n_H} + EC_{50}^{n_H}} + \frac{\text{stim}^n}{\text{stim}^n + K_S^n} \frac{k_{\text{stim}}}{1 + \left(\frac{G^*}{K_{G^*}}\right)^{n_1}}}$$

$$\frac{dM^*}{dt} = k_{\text{on}}^M M - k_{\text{off}}^M M^* - \gamma_M M^*$$

$$\frac{dG^*}{dt} = k_{\text{on}}^G \frac{(G_I - G^*)}{K_M^{n_2} + \text{stim}^{n_2}} - k_{\text{off}}^G G^*$$

The feedback model is given by

$$\frac{dM}{dt} = k_{\text{off}}^M M^* - \gamma_M M - k_{\text{on}}^M M + \frac{f_{\text{pos}} \frac{M^{*n_H}}{M^{*n_H} + EC_{50}^{n_H}} + \frac{\text{stim}^n}{\text{stim}^n + K_S^n} \frac{k_{\text{stim}}}{1 + \left(\frac{G^*}{K_{G^*}}\right)^{n_1}}}$$

$$\frac{dM^*}{dt} = k_{\text{on}}^M M - k_{\text{off}}^M M^* - \gamma_M M^*$$

$$\frac{dG^*}{dt} = k_{\text{on}}^G \frac{(G_I - G^*)}{K_M^{n_2} + M^{*n_2}} - k_{\text{off}}^G G^*$$

stim is an aggregate of all interphase signaling; *M* is newly synthesized Mos; *M\** is an aggregate of stabilized Mos and all Mos-dependent signaling; *G\** is active GSK-3 $\beta$ ; *k*<sub>on</sub> designates activation terms; *k*<sub>off</sub> designates inactivation terms;  $\gamma$  designates destruction; *n* terms are theoretical Hill coefficients. To model 7AIPM treatment (Fig. 2A), *G\** was set to zero. See also (8).

12. R. Dajani et al., *Cell* **105**, 721 (2001).
13. D. L. Fisher, N. Morin, M. Doree, *Development* **126**, 567 (1999).
14. D. H. Kim et al., *Cell* **110**, 163 (2002).
15. K. Peyrollier, E. Hajdudch, A. S. Blair, R. Hyde, H. S. Hundal, *Biochem. J.* **350**, 361 (2000).
16. T. S. Gardner, C. R. Cantor, J. J. Collins, *Nature* **403**, 339 (2000).
17. K. Amonlirdviman et al., *Science* **307**, 423 (2005).
18. G. Lahav et al., *Nat. Genet.* **36**, 147 (2004).
19. J. R. Pomeroy, S. Y. Kim, J. E. Ferrell Jr., *Cell* **122**, 565 (2005).
20. M. Acar, A. Becskei, A. van Oudenaarden, *Nature* **435**, 228 (2005).
21. O. Brandman, J. E. Ferrell Jr., R. Li, T. Meyer, *Science* **310**, 496 (2005).
22. N. T. Ingolia, A. W. Murray, *Curr. Biol.* **17**, 668 (2007).
23. G. M. Suel, J. Garcia-Ojalvo, L. M. Liberman, M. B. Elowitz, *Nature* **440**, 545 (2006).
24. We thank J. Yue for providing Mos and cyclin protein; N. L. Salimi for help with statistics; J. J. Fleming and P. M. England for help with oocytes; and A. W. Murray, R. D. Mullins, J. A. Blair, and E. C. Garner for critical reading of the manuscript. Funding from NIH grant AI49006 (to K.M.S.), the Sandler Family Supporting Foundation (to H.E.), and NIH grant GM46383 (to J.E.F.).

#### Supporting Online Material

www.sciencemag.org/cgi/content/full/324/5926/509/DC1  
Materials and Methods

Figs. S1 to S10

Tables S1 to S3

References

9 December 2008; accepted 17 March 2009

10.1126/science.1169498